Numerical diagnostic of the circulation in the Santos Bight with COROAS hydrographic data

Mauro CIRANO & Edmo J. D. CAMPOS

Instituto Oceanográfico da Universidade de São Paulo

(Caixa Postal 66149, 05389-970 São Paulo, SP, Brasil)

- ***Abstract:*** This work represents part of the analyses of the data generated during the first two mesoscale hydrographic cruises of COROAS Project: one during the Summer and the other during the Winter of 1993. The area surveyed during these cruises is the region of the South Brazil Bight (or Santos Bight) limited at the coast by the cities of Ubatuba and Iguape, extending from the 50 m isobath to oceanic regions with depths greater than 2500 m. The main goal of this work consisted of the adaptation of the *Princeton Ocean Model* to the area of study, including realistic topography, observed thermohaline structure and open boundaries. Using this model, a set of diagnostic experiments was realized using density structures based on the COROAS hydrographic data. The baroclinic velocity fields obtained, as expected from preliminary analyses of the thermohaline structures, showed similar features for the Brazil Current in both seasonal cruises. The results show an intrusion of Tropical Water over the continental shelf in the region between Ubatuba and Santos, both during the Summer and the Winter cruises. The results also suggest the penetration of the South Atlantic Central Water, underneath the Tropical Water, to the external part of the continental shelf in both occasions.

- ***Resumo:*** Este artigo representa parte das análises desenvolvidas com os dados hidrográficos coletados durante os dois primeiros cruzeiros do sub-projeto Hidrografia de Meso-escala (HM) do Projeto COROAS: o primeiro no verão e o outro no inverno de 1993. A área amostrada nos dois cruzeiros é limitada na costa pelas cidades de Iguape e Ubatuba, estendendo-se da isóbata de 50 m até regiões oceânicas com mais de 2500 m de profundidade. O objetivo central deste trabalho resumiu-se na adaptação do *Princeton Ocean Model* para a região de estudo, incluindo batimetria real, os campos termohalinos observados e contornos abertos. Usando-se esse modelo, realizou-se um conjunto de experimentos diagnósticos usando estruturas de densidade baseadas nos dados hidrográficos do COROAS. Os campos baroclínicos de correntes obtidos, de acordo com o esperado a partir de análises das estruturas termohalinas, apresentaram feições para a Corrente do Brasil bastantes similiares em ambos os cruzeiros. Esses resultados sugerem uma intrusão da Água Tropical sobre a plataforma continental na região entre Ubatuba e Santos, tanto durante o cruzeiro de verão quanto no de inverno. Os resultados sugerem, também, penetração da Água Central do Atlântico Sul sobre a plataforma nas duas ocasiões.

- ***Descriptors:*** Brazil Current, thermohaline structure, Santos Bight, σ-coordinate.

- ***Descritores:*** Corrente do Brasil, estrutura termohalina, Bacia de Santos, coordenadas sigma.

Introduction

The large-scale circulation in the South Atlantic ocean has been relatively well investigated since the *Meteor* expedition in the 1920's. However, until recently most of the oceanographic studies in that part of the ocean were aimed at the general aspects of the circulation, of the main patterns of temperature and salinity fields, and of the characteristic water masses (Reid *et al.*, 1977; Garfield III, 1990; Peterson & Stramma, 1991). At the mesoscale, several studies had been developed in the past twenty years or so (*e.g.:* Signorini, 1976, 1978; Miranda & Castro Filho, 1979, 1982; Evans *et al.*, 1983; Miranda, 1985; Signorini *et al.*, 1989; Campos *et al.*, 1994, 1995), but in general, these studies were concentrated in specific regions, mainly between Cabo de São Tomé and Rio de Janeiro.

With the advent of the recent international programs, such as the World Ocean Circulation Experiment (WOCE), the oceanographic community started to look more intensively at the smaller scale features, especially in the western region of the ocean near the coastline of South America. In this respect, one of the first Brazilian research efforts to look at mesoscale processes in the Brazil Current (BC) region following the strict WOCE specifications is the COROAS (Circulação Oceânica na Região Oeste do Atlântico Sul or Oceanic Circulation in the Western Region of the South Atlantic) experiment (Cirano, 1995; Silva, 1995; Ikeda & Campos, 1995; Campos, 1995).

One component of the COROAS project is a mesoscale hydrographic (HM) survey of the South Brazil or Santos Bight region between 23° and 27°S, encompassing the continental shelf and the adjacent deep ocean. This study was carried out during three oceanographic cruises on board the University of São Paulo's *R/V W. Besnard*, the first (HM1) from Jan/22 to Feb/04/93; the second (HM2) from Jul/15 to Jul/29/93; and the third (HM3) from Jan/15 to Jan/29/94. During each of these cruises, approximately one hundred hydrographic stations for CTD (*Conductivity-Temperature-Depth)* profiling were occupied. Figure 1 shows the location of these stations during the first two cruises (HM1 and HM2), data of which are analyzed in the present work.

In this article, the thermohaline data obtained during HM1 and HM2 is used to initialize a diagnostic implementation of the *Princeton Ocean Model* (POM) to the region surveyed, in a study of the flow associated with the observed mass field. The rationale for this approach is that the chosen numerical model (POM) uses the full momentum equation to compute the velocity field, while the classical geostrophic approaches, such as the dynamical method, employ only two terms: Coriolis and pressure gradient. Consequently, one would expect that results produced by the numerical model should be more realistic.

The Brazil Current Features in the Area of Study

The Brazil Current originates at the bifurcation of South Equatorial Current and flows southwards along the Brazilian coast to the Subtropical Convergence, at approximately 38°S (Peterson & Stramma, 1991). Compared with its North Atlantic counterpart (the Gulf Stream), the BC presents a much weaker volume transport, which is explained by Stommel (1965) to be a consequence of the opposite directions of wind-driven and thermohaline flows in the subtropical South Atlantic. The actual transport values, mainly estimated from hydrographic data, are in general up to 10-12 Sv in the region of the Santos Bight (Campos *et al.*, 1995).

The thermohaline structure of the Brazil Current is composed by two water masses flowing southwards: the warm salty Tropical Water (TW) (Emilsson, 1961), with temperatures T $>$ 20°C and salinities S $>$ 36, flowing above the pycnocline; and the South Atlantic Central Water (SACW) (Sverdrup *et al.*, 1942; Thomsen, 1962; Miranda, 1985), which flows to the south within the thermocline region, with 6°C $<$ T $<$ 20°C and 34.6 $<$ S $<$ 36. According to the classical picture, below the Brazil Current, in increasing depth, the water masses are those represented by the Antarctic Intermediate Water (AAIW): 3°C $<$ T $<$ 6°C and 34.2 $<$ S $<$ 34.6; the North Atlantic Deep Water (NADW): 3°C $<$ T $<$ 4°C and 34.6 $<$ S $<$ 35; and the Antarctic Bottom Water (AABW), waters with temperature T $<$ 3°C and salinities S $<$ 35.

The present knowledge of the BC is based mainly in results of geostrophic calculations with observed thermohaline data obtained with Nansen bottles. Only recently CTD probes have been used in the region (Campos *et al.*, 1994, 1995) and very few direct measurements have been performed so far. Numerical data are mainly from a few regional models or from global models with poor resolution. Among these studies, Mellor *et al.* (1982) computed the Ekman, thermohaline and bottom transports in a global model which barely resolved mesoscale features near the South American coast. Campos & Olson (1991), using a basin scale implementation of an isopycnic coordinate model described the Brazil Current as a low transport current with mesoscale eddies as energetic as those observed in the Gulf Stream. Climatological annual mean values of temperature and salinity of Levitus (1982), and the climatological wind stress data of Hellerman and Rosenstein (1983) have been used by Semtner & Chervin (1988) and Matano & Philander (1993) in global and basin-scale models with somewhat good resolution of mesoscale processes in the region focused on the present paper. However, specific mesoscale implementations of "state-of-the-art" models, such as the one discussed here, are practically nonexistent in the literature. The regional numeric models applied for this specific area are represented by Harari (1984), Castro Filho (1995), Lorenzzetti *et al.* (1988) and Stech (1989). These models fail to describe accurately the Brazil Current, because they are either barotropic or linear.

Material and Methods

The hydrographic data

As seen in Figure 1, the coastline in the region of study is oriented almost in the NE-SW direction. In that region, the Brazil Current is usually found near the shelf break (200 m isobath), meandering in a very energetic pattern, probably due to the abrupt change in coastline direction near Cabo Frio (RJ). The HM transects were planned to be approximately perpendicular to the shelf break in order to explore the geostrophy of the along-isobath component

of the flow, but with a reasonable distance between consecutive transects (approximately 50 km) for resolving also the along-isobath variability. Each transect extended from the 50 m isobath to regions with depth of the order of 2500 m. The stations along each of the seven transects of Figure 1 were spaced approximately 17 km apart, except near the shelf break, where a 10 km spacing was adopted for better resolution of the complex dynamics of the region. In each station a CTD probe was used to collect information on the thermohaline structure of the water column. The temperature and salinity data obtained in each of these stations were used to compute water density.

The Numerical Model

As indicated in the introduction, the central idea of this work is to use a numerical model, in diagnostic mode, to obtain the baroclinic velocities associated with the observed mass field. The model employed is the σ-coordinate POM (Blumberg & Mellor, 1987; Mellor, 1993), which is particularly suited for modelling regions with strong bathymetric gradients, such as the shelf break and slope regions. The POM is a three-dimensional, primitive equation model, using a second-moment turbulence closure scheme (Mellor & Yamada, 1982) to give more realistic surface and bottom Ekman layers.

For the experiments reported in this article, the model was adapted to the region, including the real bottom topography, in a grid covering the area surveyed by the oceanographic cruises HM1 and HM2 (Figure 1). The origin of the x-y coordinate system was placed at (47° 33' W, 24° 42' S) and the axes were rotated by an angle of 45°, in order to have the y-axis oriented approximately in the alongshore direction. The *β-plane* approximation was used and the grid points were equally spaced in the horizontal, with a 10 km grid spacing. Horizontally, the domain dimensions were 300 km in the y direction and 350 km in the x direction. In the vertical, 18 σ–levels were used (Table 1), with exponential distribution in the uppermost five levels and linear distribution in the remaining ones. Regions with depths less than 50 m were considered dry areas while depths greater than 2000 m were reduced to 2000 m. For this spatial setting, the CFL (Courant-Friedrichs-Levy) criterion suggests, for

the barotropic mode, a maximum time step interval of 25 s (the model integrates separately the external and internal modes). The effective value, however, was focused to be 15 s. The corresponding internal time step, used to upgrade the baroclinic modes, was equal to 300 s. In all experiments, the Smagorinsky's formulation (Smagorinsky, 1963) was used for horizontal diffusion, the local grid size and the velocity gradients are used to calculate the horizontal diffusivity.

The hydrographic (temperature and salinity) data collected during the first two COROAS mesoscale cruises were interpolated to each point of the model's three dimensional grid and a set of experiments was run in the diagnostic mode. That is, the mass structure was kept constant all the time, while the velocity field, spun up from rest, eventually adjusted to this prescribed thermohaline distribution.

Boundary Conditions

A common problem in limited-area implementations of numerical models is the proper specification of boundary conditions. These conditions, which should "transmit" to the area under investigation the effects of remote forcings, are usually in the form of prescribed fluxes, thermohaline distribution and sea surface elevation. In the present case, since the thermohaline field is kept constant during all the experiments, the boundary conditions were taken from an assumed total barotropic volume transport across the open boundaries and associated sea surface elevation.

For the sea surface elevation, the gradient condition was used, eliminating the gradient of the surface height across the boundaries. The dynamic effect of this condition is the elimination of the geostrophic velocity parallel to the boundary, at the boundary points. For the normal component of the external velocity, in some of the experiments an imposed mass inflow/outflow was prescribed. This procedure was used because the main interest was the baroclinic field, which is obtained subtracting the barotropic field from the total one.

Assuming that the barotropic field exchanges little energy with the baroclinic field, then this approach would be reasonable. Thus, in order to test the validity of this assumption, experiments with different barotropic fields were carried out. For each cruise, the model was run with two different values of the barotropic volume transport across the open boundaries: 10 Sv and 0 Sv. The associated velocity distribution (in the case of 10 Sv) along the north and south boundaries are shown in Figure 2.

For the tangential component of the external and internal velocities, boundary conditions were applied only for the non-linear advective terms. For the normal component of the internal mode of the velocity, a Sommerfeld-like radiative condition (Sommerfeld, 1949) was applied. This condition is described as a gravity-wave radiative condition (Chapman, 1985).

Model Initialization

In this article four experiments are discussed. They were carried out with the objective of, first, to compare the methodology adopted, and second, to evaluate the seasonality between the HM1 and HM2 cruises. For each cruise, two experiments were done, one with prescribed mass inflow/outflow, and another with no flow across the open boundaries. The two first experiments, labeled EXP1 (with inflow/outflow) and EXP2 (with no inflow/outflow), refer to the summer cruise (HM1). The last two, EXP3 (with inflow/outflow) and EXP4 (without flow across the boundaries), refer to the winter cruise (HM2). The Table 2 summarizes the experiments.

Part of the thermohaline structures used in the model initialization are shown in vertical profiles for both HM1 (Figure 3) and HM2 (Figure 4). In these figures, the upper panel represents the northern part of the domain, the middle one shows transect in the central part, and the lower one represents the southern boundary.

In all experiments (EXP1 through EXP4) the model was allowed to run for 15 simulation days. The time-history of the basin-averaged kinetic energy during the four runs are shown

in Figure 5. In all cases the model reached an equilibrium state after approximately five simulation days.

Results

The summer cruise - HM1

Based on a crude analysis of the thermohaline structure along Transect 1 (Figure 3), according to the values of water properties proposed by Miranda (1985), one would expect to find the Brazil Current front located near the coast; the Tropical Water occupying the upper 150 m, in oceanic regions; and the SACW in the thermocline region, below 150 m of depth. It also seems to be clear, from the upper panel of Figure 3, that there is a core of SACW in the continental shelf region, near the bottom, which is not connected to the water with the same characteristics in the deeper oceanic region. On Transect 4 (middle panel of Figure 3), the Brazil Current front is not so close to the coast, but one could still identify the same core of SACW over the shelf, separated from the oceanic one by the Brazil Current front. In the southern part of the domain (lower panel of Figure 3), with the Brazil Current front located farther from the coast, one can notice that now there is a clear connection between the SACW located over the shelf and that located in oceanic regions.

For the HM1 experiments (EXP1 and EXP2), vertical profiles of velocity (Figure 6) are shown for the same transects discussed above. Using the -0.1 ms^{-1} isoline as the lower bound for the Brazil Current velocity, it is observed that on Transect 1 (upper panel of Figure 6) the Brazil Current front is clearly located near the coast, with its core inshore of the shelf break, reaching depths of 100 m. On the middle transect (middle panel of Figure 6), the main core of the current is now located near the continental slope reaching depths down to 350 m. On the southernmost transect (lower panel), the Brazil Current core is found farther offshore, and reaches depths of approximately 500 m.

The horizontal profiles of the velocity field produced by the numerical experiments for the surface and the depths of 100 m, 200 m and 500 m, are presented for EXP1 (Figure 7) and EXP2 (Figure 8). In these vector plots, one can observe, as suggested by the thermohaline structure, the Brazil Current penetrating in the area surveyed from the northeast, along a direction almost perpendicular to the shelf break. After reaching the 200 m isobath, however, the flow turns southward, meandering around the shelf break. The highest velocity values for the current are located in the upper 200 m. In the lower regions, the velocity decreases monotonically down to 500 m. Between 500 m and 700 m there seems to be a change in the velocity orientation, which may represent the AAIW flow to the north.

The winter cruise - HM2

The thermohaline structures for HM2 (Figure 4) show patterns similar to those from the HM1, especially regarding the location of the Brazil Current front. That is, the front is located nearer to the coast on the northernmost transect and farther into the ocean in the southernmost one. The TW, on Transect 1 is limited to the regions above 120 m, in oceanic regions, with water with characteristics of SACW below that level, in the thermocline. Penetration of SACW onto the shelf is also observed, with no connection between the continental shelf SACW and the oceanic SACW, again associated with the position of the Brazil Current front. On Transect 6, when the front is far from the coast, the SACW penetrates more freely onto the shelf, in comparison with transect 1, where the front is located more inshore.

On the continental shelf, for Transects 1 and 4, the temperature field is quite homogeneous, without the strong seasonal thermocline observed during the summer cruise (upper and middle panels of Figure 4). On Transect 6 (lower panel of Figure 4), however, a thermocline is observed. This seems to be associated with the SACW penetration and the presence of a cooler mass of water coming into the domain from the south. Notably, this feature is also observed in the salinity field, already on Transect 4 (Figure 4). A strong salinity gradient is observed in the upper layers of the shelf. This gradient, showing low salinity waters near the coast, is clearly not related to the SACW penetration and seems to confirm the penetration

of a coastal water coming from the south and flowing northward.

The velocity fields in EXP3 and EXP4, in analogy with the results found in HM1, show a Brazil Current intensifying and reaching greater depths as it flows to the south. On Transect 1 (Figure 9), the main core of the current is located near the shelf and limited to the upper 100 m. On the central transect (middle panel of Figure 9), the main core of the current is located over the continental slope, reaching depths of 360 m. On the southernmost transect (lower panel of Figure 9), the current is most intense, and its core reaches to depths of 450 m.

The horizontal velocity fields show a well marked current, as found in the results of the HM1 experiments. The horizontal velocity fields have the highest values in the upper 100 m, in both EXP3 (Figure 10) and EXP4 (Figure 11).

Discussion

Except for the seasonal differences observed either in the thermohaline structure and in the velocity fields, a clear similarity was observed in the general results of HM1 and HM2. In both cases, a similar pattern for the Brazil Current was obtained, with the presence, in the two kinds of experiments for each cruise, of a cyclonic meander in the study area. As part of this meandering pattern, the current front is observed nearer to the coast in the vicinity of Ubatuba and farther into the ocean in the southern part of the domain.

In both cruises, the SACW penetration onto the shelf observed is probably due to the mechanism proposed by Campos *et al.* (1995), and seems to be associated with the cyclonic meandering of the Brazil Current; a topographic Rossby wave apparently induced by the upstream change in the coastline orientation.

Regarding the thermohaline structure, a pronounced thermocline in the shelf region is observed during the summer and in all transects of HM1 (Figure 3)[see also Matsuura (1986)].

However, the expected wintertime homogeneous shelf water reported by Matsuura (1986) could only be observed in Transects 1 and 4 (Figure 4). In Transect 6, in a different pattern, a thermocline could be observed also in the winter of 1993 cruise.

Conclusion

From the results above, we find that the results with or without the imposed mass inflow/outflow are very similar and show the same general features. This agreement suggests that the barotropic and baroclinic fields are relatively independent from each other.

Another important conclusion is related with the penetration of the Brazil Current onto the continental shelf. This feature is present in the observed thermohaline structure and was also reproduced by the numerical experiments, in both cruises and in a similar way. The results also indicate that the current penetrates in the northern part of the domain, almost perpendicular to the coast, reaches the shelf break and invades the outer regions of the continental shelf. Due to potential vorticity conservation, the flow then turns back towards the ocean and starts to meander around the shelf break as it continues to the south. From the 1993 data analyzed here, no seasonal character of the Brazil Current penetration as found by Matsuura (1986) was apparent.

Based on the velocity fields produced by the numerical calculations and on the observed thermohaline structures in both cruises, the meandering behavior of the Brazil Current is probably linked with the change in the orientation of the coastline in the Cabo Frio (RJ) region. The current is turned westward across isobaths, as explained by Campos (1995). The results here, which relate the meandering to penetration of the SACW onto the continental shelf, also agree with Campos *et al.* (1995). The vertical profiles for thermohaline structures show that when the Brazil Current front is closer to the coast (Transect 1), the SACW observed near the bottom of the shelf is not linked with the SACW in adjacent oceanic regions for both cruises (Figure 3 and 4). On the other hand, when the current is farther

from the coast, on Transect 6, the SACW is found entirely connected with the deep ocean to the shelf region.

Acknowledgements: The authors would like to express their gratitude to Dr. Jerry L. Miller (NRL/SSC) for his valuable help in the implementation of the POM for the simulations discussed in this paper. Project COROAS was funded by Fundação de Amparo à Pesquisa do Estado de São Paulo (FAPESP) – Proc. 91/0542-7, and by Conselho Nacional de Desenovolvimento Científico e Tecnológico (CNPq) – Proc. 40.3007/91-7.

References

BLUMBERG, A. F. & MELLOR, G. L. 1987. A Description of a Three-Dimensional Coastal Ocean Circulation Model, In: HEAPS, N. S. *Three Dimensional Coastal Ocean Models, Coastal and Estuarine Sciences*, **4**. Washington, D. C., American Geophysical Union, p. 1-16.

CAMPOS, E. J. D. 1995. Estudos da Circulação Oceânica no Atlântico Tropical e na Região Oeste do Atlântico Subtropical Sul. Postdoctoral Thesis, Univ. of São Paulo, 114 pp.

CAMPOS, E. J. D. & OLSON, D. B. 1991. Stationary Rossby Waves in Western Boundary Currents Extensions. *J. phys. Oceanogr.*, **21(8)**, 1202-1224.

CAMPOS, E. J. D.; GODOI, S. S.; IKEDA, Y.; NONATO, L. V. & GONÇALVES, J. E. 1994. Summertime thermohaline structure of the Brazil Current Region between Santos (SP) and Rio de Janeiro (RJ). *Bolm Inst. oceanogr.*, S. Paulo, **42(1/2)**, 1-18.

CAMPOS, E. J. D.; GONÇALVES, J. E. & IKEDA, Y. 1995. Water mass characteristics and geostrophic circulation in the South Brazil Bight: Summer of 1991. *J. Geophys. Res.*, **100**, 18537-18550.

CASTRO FILHO, B. M. 1985. Subtidal response to wind forcing in the South Brazil Bight during winter. Ph.D. Thesis, Univ. of Miami, 211 pp.

CHAPMAN, D. C. 1985. Numerical Treatment of Cross-Shelf Open Boundaries in a Barotropic Coastal Ocean Model. *J. phys. Oceanogr.*, **15**, 1060-1075.

CIRANO, M. 1995. Utilização de Modelo Numérico no Estudo Diagnóstico da Circulação Oceânica na Bacia de Santos. M.S. thesis, Univ. of São Paulo, 116 pp.

EMILSSON, I. 1961. The Shelf and Coastal Waters off Southern Brazil. *Bolm Inst. oceanogr.*, S. Paulo, **11**, 101-112.

EVANS, D. L.; SIGNORINI, S. R. & MIRANDA, L. B. 1983. A Note on the Transport of the Brazil Current. *J. phys. Oceanogr.*, **13**, 1732-1738.

GARFIELD III, N. 1990. The Brazil Current at Subtropical Latitudes. Ph.D. Thesis, Univ. of Rhode Island, 121 pp.

HARARI, J. 1984. Modelo numérico hidrodinâmico tri-dimensional linear da plataforma continental sudeste do Brasil. Ph.D. Thesis, Univ. of São Paulo, 203 pp.

HELLERMAN, S. & ROSENSTEIN, M. 1983. Normal Monthly Wind Stress Over the World Ocean with Error Estimates. *J. phys. Oceanogr.*, **13**, 1093-1104.

IKEDA, Y. & CAMPOS, E. J. D. 1995. Oceanic Circulation in Western Region of the South Atlantic - The COROAS Experiment. *Reports of Governing and Major Subsidiary Bodies*, **IOC-WMO/IWP-III/3 Annex VI**, 8-11.

LEVITUS, S. 1982. Climatological atlas of the world ocean. NOAA Prof. Paper 13, U. S. Govt. Printing Office, Washington, D. C., 173 pp.

LORENZZETTI J. A.; TANAKA, K. & WANG, J. D. 1988. Simulação numérica da ressurgência costeira em Cabo Frio (RJ) através de um modelo em elementos finitos de duas camadas. São José dos Campos, INPE, (INPE-4502-RPE/561)

MATANO, R. P. & PHILANDER, S. G. H. 1993. Heat and Mass balances of the South Atlantic Ocean calculated from a numerical model. *J. Geophys. Res.*, **98 (C1)**, 977-984.

MATSUURA, Y. 1986. Contribuição ao estudo da estrutura oceanográfica da região sudeste entre Cabo Frio (RJ) e Cabo de Santa Marta Grande (SC). *Ciência e Cultura* , **38(8)**, 1439-1451.

MELLOR, G. L. 1993. *User's Guide for A Three-Dimensional, Primitive Equation, Numerical Ocean.* New Jersey, Atmospheric and Oceanic Sciences Program, Princeton University, 35 pp.

MELLOR, G. L.; MECHOSO, C. R. & KETO, E. 1982. A diagnostic calculation of the general circulation of the Atlantic Ocean. *Deep-Sea Res.*, **29(10A)**, 1171-1192.

MELLOR, G. L. & YAMADA, T. 1982. Development of a Turbulence Closure Model for Geophysical Fluid Problems. *Revs of Geophys. Space Phys.*, **20**, 851-875.

MIRANDA, L. B. 1985. Forma da Correlação T-S de Massas de Água das Regiões Costeira e Oceânica entre o Cabo de São Tome (RJ) e a Ilha de São Sebastião (SP), Brasil. *Bolm Inst. oceanogr.*, S. Paulo, **33(2)**, 105-119.

MIRANDA, L. B. & CASTRO FILHO, B. M. 1979. Condições de Movimento Geostrófico das Águas Adjacentes a Cabo Frio (RJ). *Bolm Inst. oceanogr.*, S. Paulo, **28(2)**, 79-93.

MIRANDA, L. B. & CASTRO FILHO, B. M. 1982. Geostrophic Flow Conditions of the Brazil Current at 19° S. *Ciência interamer.* , **22(1/2)**, 44-48.

PETERSON, R. G. & STRAMMA, L. 1991. Upper-level circulation in the South Atlantic Ocean. *Prog. Oceanogr.*, **26(1)**, 1-73.

REID, J. L.; NOWLIN, W. D. & PATZERT, W. C, 1977. On the Characteristics and Circulation of the Southwestern Atlantic Ocean. *J. phys. Oceanogr.*, **7**, 62-91.

SEMTNER, A. J. & CHERVIN, R. M. 1988. A simulation of the Global Ocean Circulation with resolved eddies. *J. Geophys. Res.*, **93 (C12)**, 15502-15522.

SIGNORINI, S. R. 1976. Contribuição ao Estudo da Circulação e do Transporte de Volume da Corrente do Brasil entre o Cabo de São Tomé e a Baia de Guanabara. *Bolm Inst. oceanogr.*, S. Paulo, **25**, 157-220.

SIGNORINI, S. R. 1978. On the circulation and the volume transport of the Brazil Current between the Cape of São Tome and Guanabara Bay. *Deep-Sea Res.*, **25**, 481-490.

SIGNORINI, S. R.; MIRANDA, L. B.; EVANS, D. L.; STEVENSON, M. R. & INOSTROZA, H. M. 1989. Corrente do Brasil: estrutura térmica entre 19° e 25° S e circulação geostrófica. *Bolm Inst. oceanogr.*, S. Paulo, **37(1)**, 33-49.

SILVA, M. P. 1995. Caracterização fisico-química das massas de água da Bacia de Santos durante o projeto COROAS. Verão e Inverno de 1993. M.S. thesis, Univ. of São Paulo, 135 pp.

SMAGORINSKY, J. 1963. General circulation experiments with the primitive equations, I. The basic experiment. *Mon. Weath. Rev.*, **91**, 99-164.

SOMMERFELD, A. J. 1949. *Partial differential equations in physics.* New York, Academic Press, 335 pp.

STOMMEL, H. 1965. *The Gulf Stream. A physical and dynamical description.* 2nd Ed., University of California Press, Berkeley, 248 pp.

STECH, J. L. 1989. Um estudo comparativo da dinâmica da circulação de inverno entre as plataformas continentais das costas sudeste do Brasil e dos Estados Unidos utilizando um modelo numérico. Ph.D. Thesis, Univ. of São Paulo, 224 pp.

SVERDRUP, H. U.; JOHNSON, M. W. & FLEMING, R. H. 1942. *The Oceans: Their Physics, Chemistry and General Biology.* Englewood Cliffs, New Jersey, Prentice Hall, 1087 pp.

THOMSEN, H. 1962. Massas de Agua Caracteristicas del Oceano Atlantico - Parte Sudoeste. *Servicio de Hidrografia Naval*, Buenos Aires, Publico, **H-632**, 1-27.

List of Figures

List of Tables

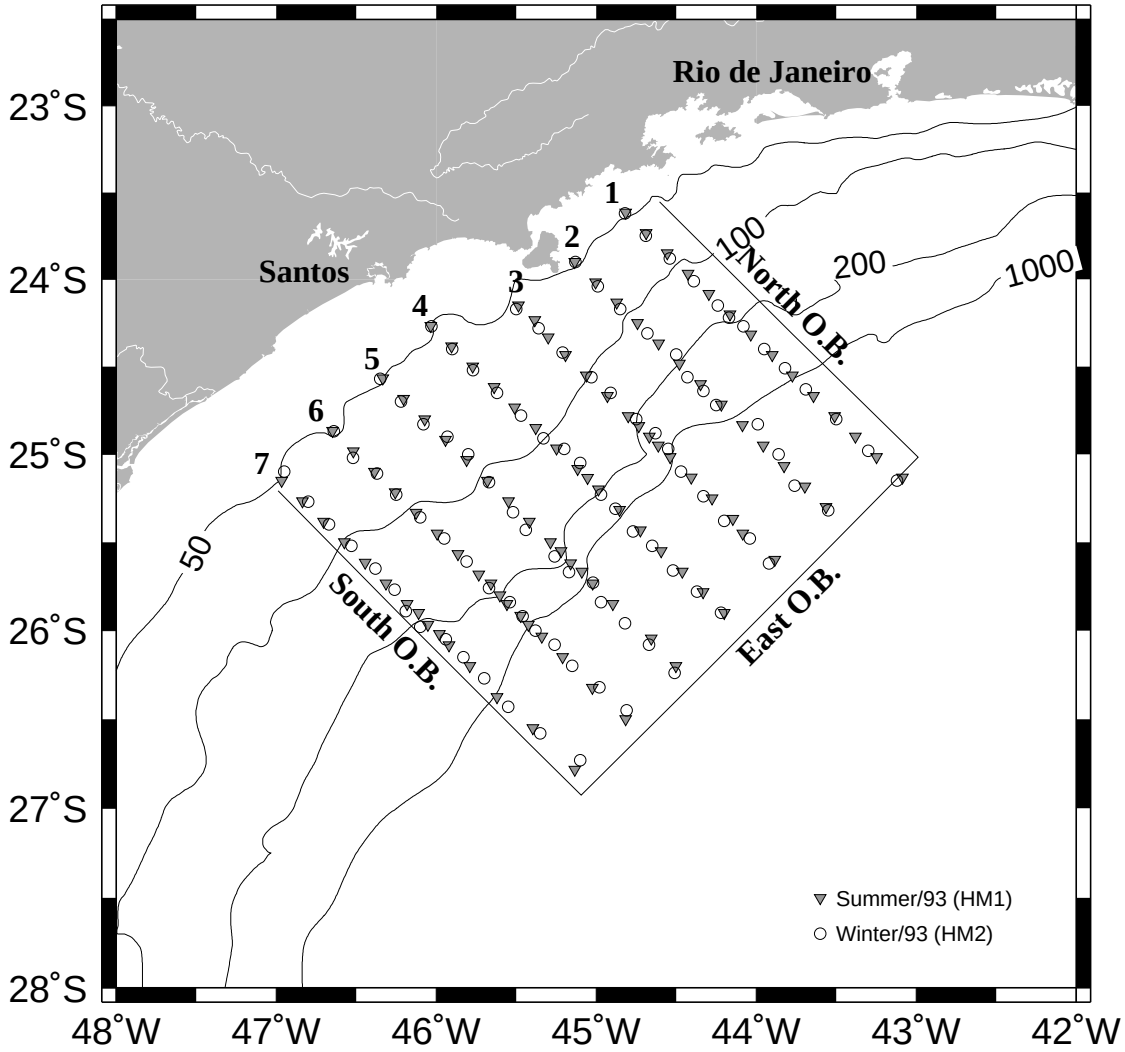
Rio de Janeiro
Santos
1
2
3
4
5
6
7
100
200
1000
50
North O.B.
South O.B.
East O.B.
Summer/93 (HM1)
Winter/93 (HM2)
23˚S
24˚S
25˚S
26˚S
27˚S
28˚S
48˚W
47˚W
46˚W
45˚W
44˚W
43˚W
42˚W

Figure 1:

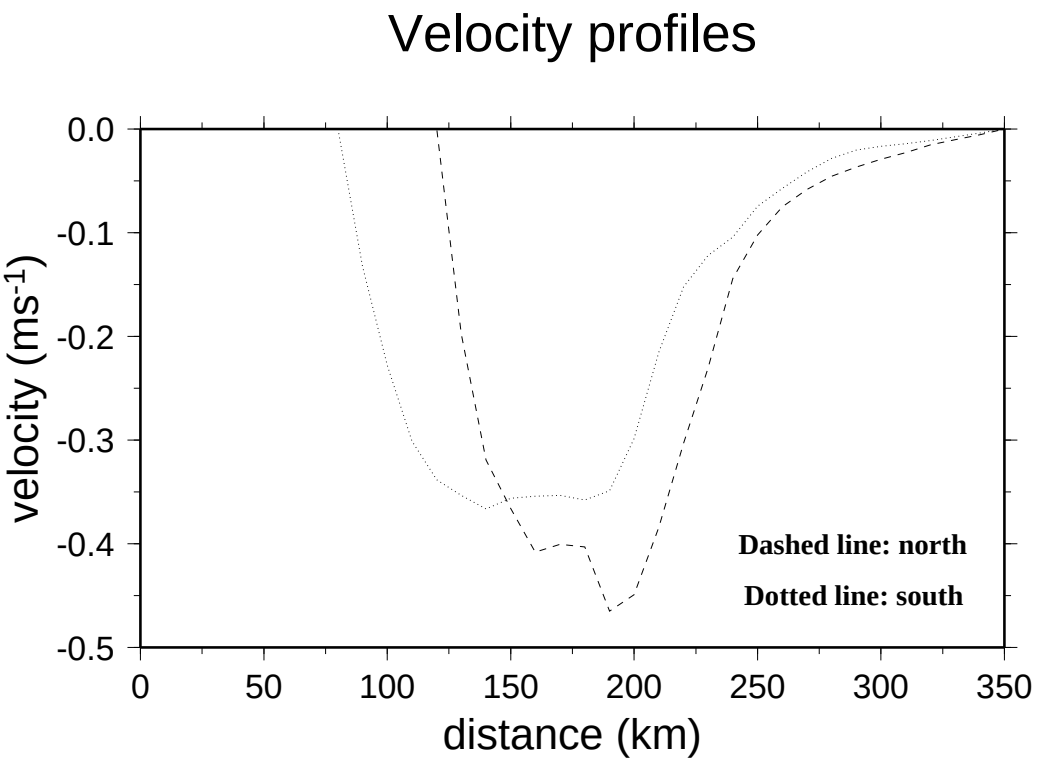
Velocity profiles
0.0
-0.1
-0.2
-0.3
-0.4
-0.5
velocity (ms-1)
0
50
100
150
200
250
300
350
distance (km)
Dashed line: north
Dotted line: south

Figure 2:

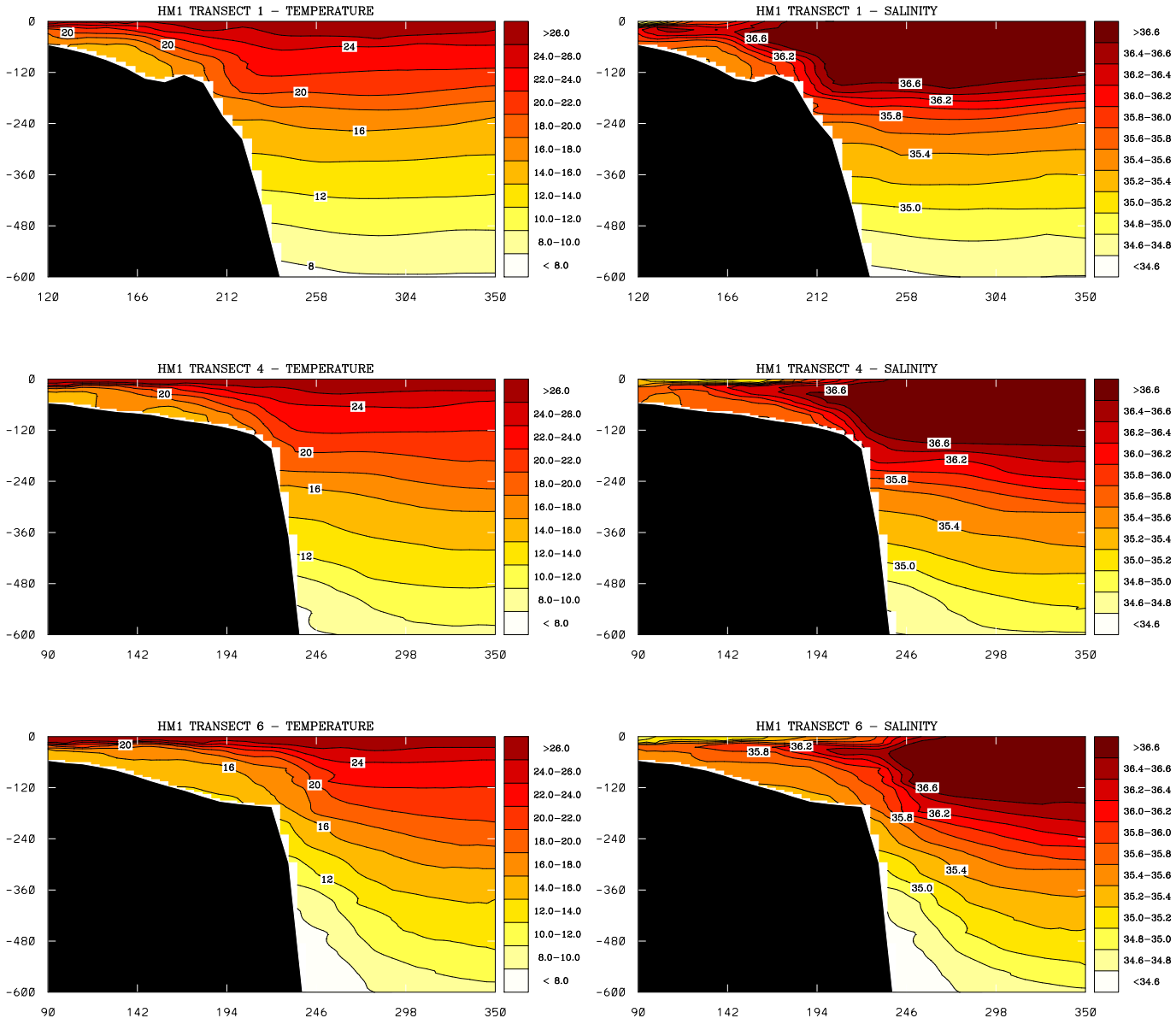
HM1 TRANSECT 1 – TEMPERATURE
HM1 TRANSECT 1 – SALINITY
HM1 TRANSECT 4 – TEMPERATURE
HM1 TRANSECT 4 – SALINITY
HM1 TRANSECT 6 – TEMPERATURE
HM1 TRANSECT 6 – SALINITY
0
-120
-240
-360
-480
-600
120
166
212
258
304
350
90
142
194
246
298
>26.0
24.0–26.0
22.0–24.0
20.0–22.0
18.0–20.0
16.0–18.0
14.0–16.0
12.0–14.0
10.0–12.0
8.0–10.0
< 8.0
>36.6
36.4–36.6
36.2–36.4
36.0–36.2
35.8–36.0
35.6–35.8
35.4–35.6
35.2–35.4
35.0–35.2
34.8–35.0
34.6–34.8
<34.6

Figure 3:

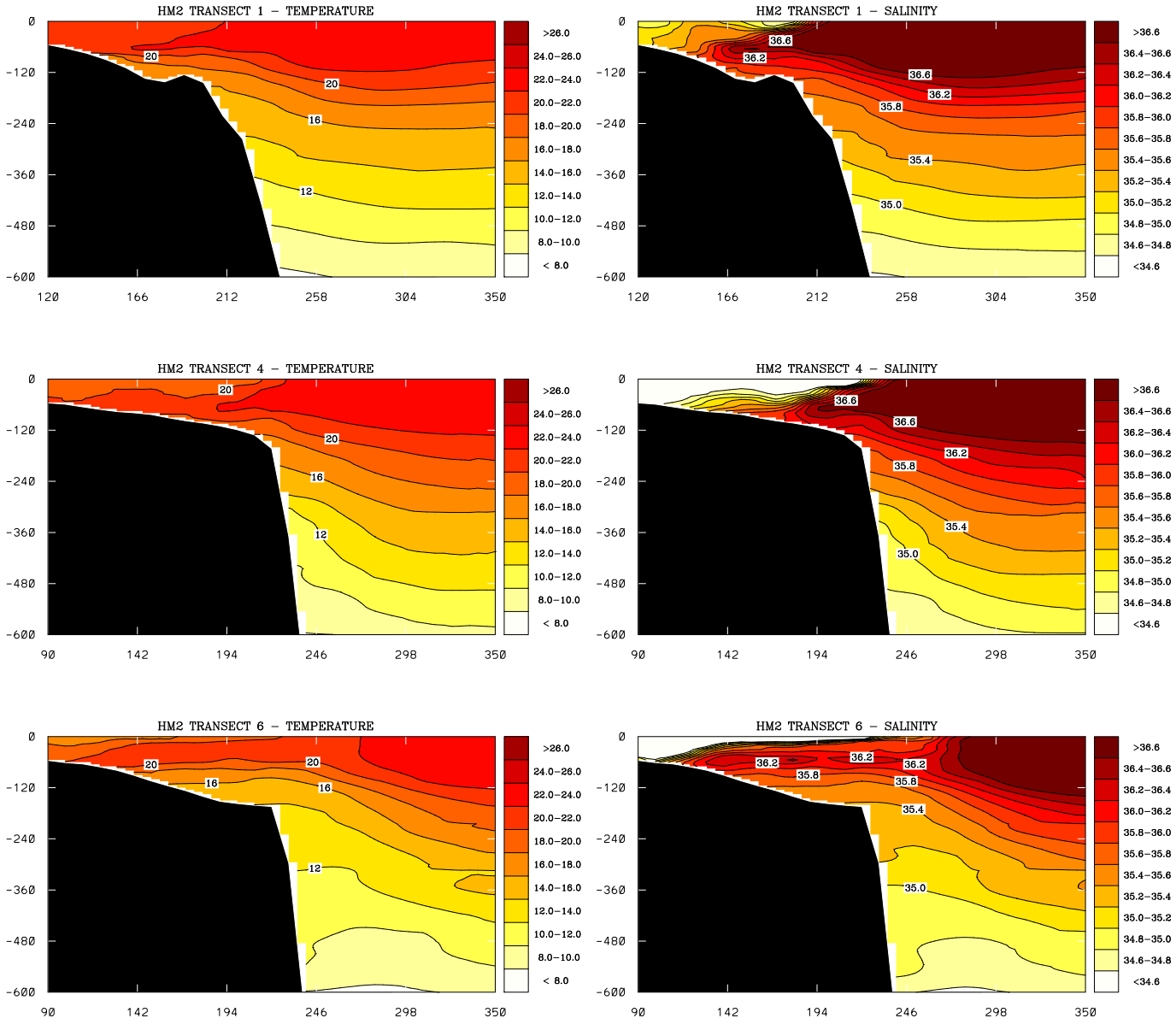
HM2 TRANSECT 1 – TEMPERATURE
HM2 TRANSECT 1 – SALINITY
HM2 TRANSECT 4 – TEMPERATURE
HM2 TRANSECT 4 – SALINITY
HM2 TRANSECT 6 – TEMPERATURE
HM2 TRANSECT 6 – SALINITY
0
-120
-240
-360
-480
-600
120
166
212
258
304
350
90
142
194
246
298
>26.0
24.0–26.0
22.0–24.0
20.0–22.0
18.0–20.0
16.0–18.0
14.0–16.0
12.0–14.0
10.0–12.0
8.0–10.0
< 8.0
>36.6
36.4–36.6
36.2–36.4
36.0–36.2
35.8–36.0
35.6–35.8
35.4–35.6
35.2–35.4
35.0–35.2
34.8–35.0
34.6–34.8
<34.6

Figure 4:

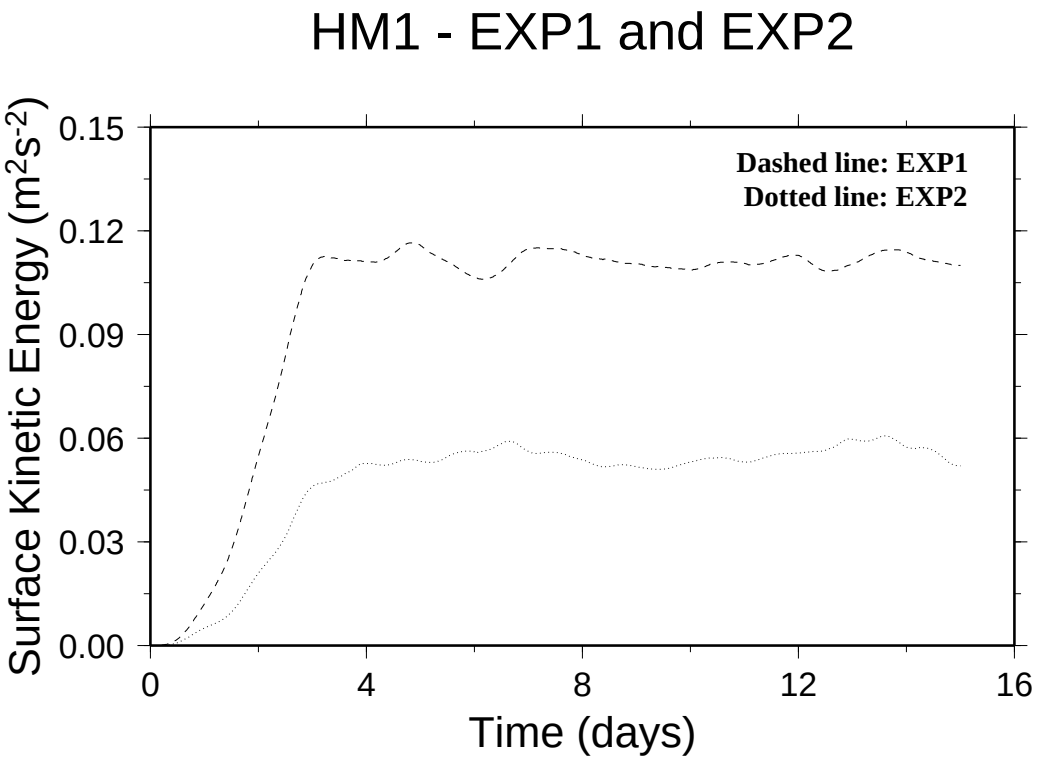
HM1 - EXP1 and EXP2
Surface Kinetic Energy (m2s-2)
0.15
0.12
0.09
0.06
0.03
0.00
Dashed line: EXP1
Dotted line: EXP2
0
4
8
12
16
Time (days)

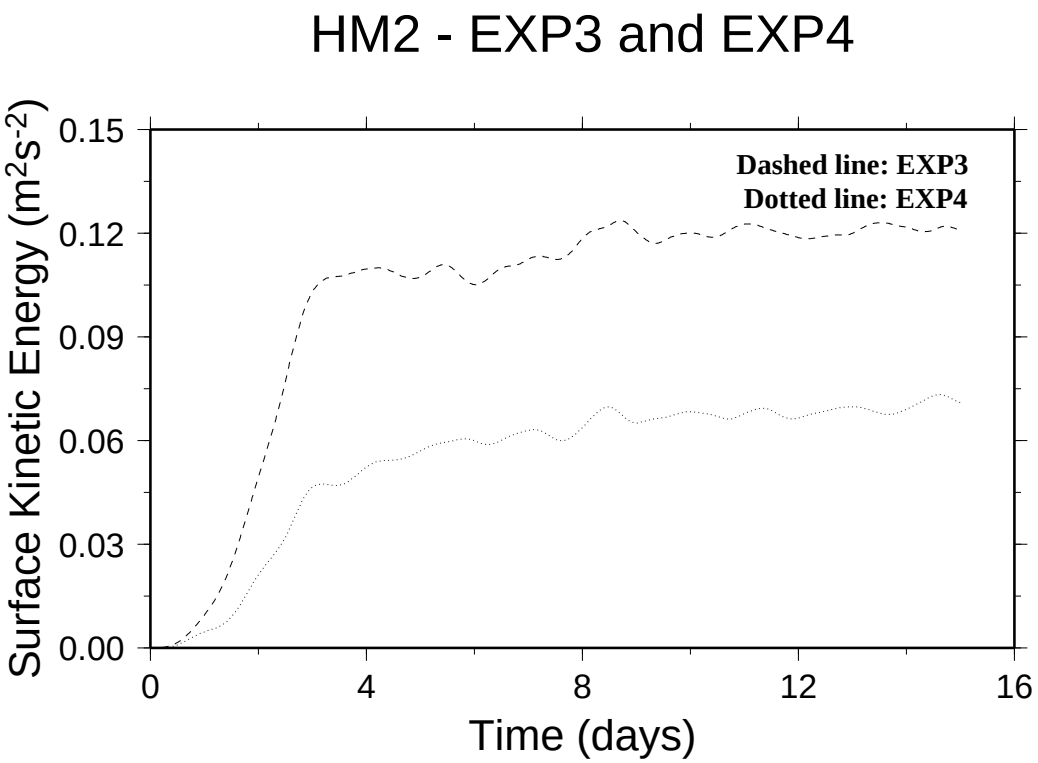
HM2 - EXP3 and EXP4
Surface Kinetic Energy (m2s-2)
0.15
0.12
0.09
0.06
0.03
0.00
Dashed line: EXP3
Dotted line: EXP4
0
4
8
12
16
Time (days)

Figure 5:

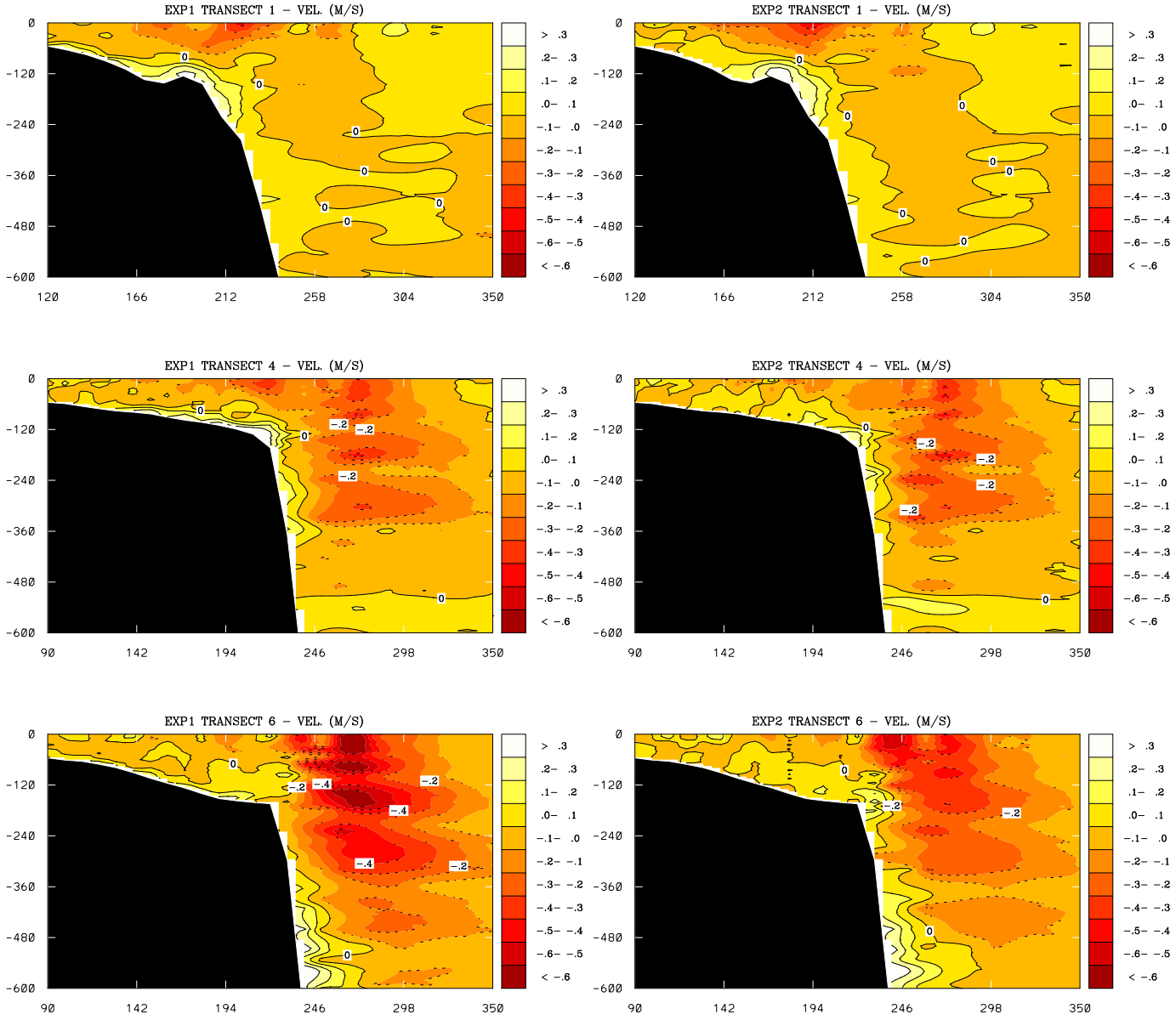
EXP1 TRANSECT 1 – VEL. (M/S)
EXP2 TRANSECT 1 – VEL. (M/S)
EXP1 TRANSECT 4 – VEL. (M/S)
EXP2 TRANSECT 4 – VEL. (M/S)
EXP1 TRANSECT 6 – VEL. (M/S)
EXP2 TRANSECT 6 – VEL. (M/S)
0
-120
-240
-360
-480
-600
120
166
212
258
304
350
90
142
194
246
298
> .3
.2– .3
.1– .2
.0– .1
–.1– .0
–.2– –.1
–.3– –.2
–.4– –.3
–.5– –.4
–.6– –.5
< –.6

Figure 6:

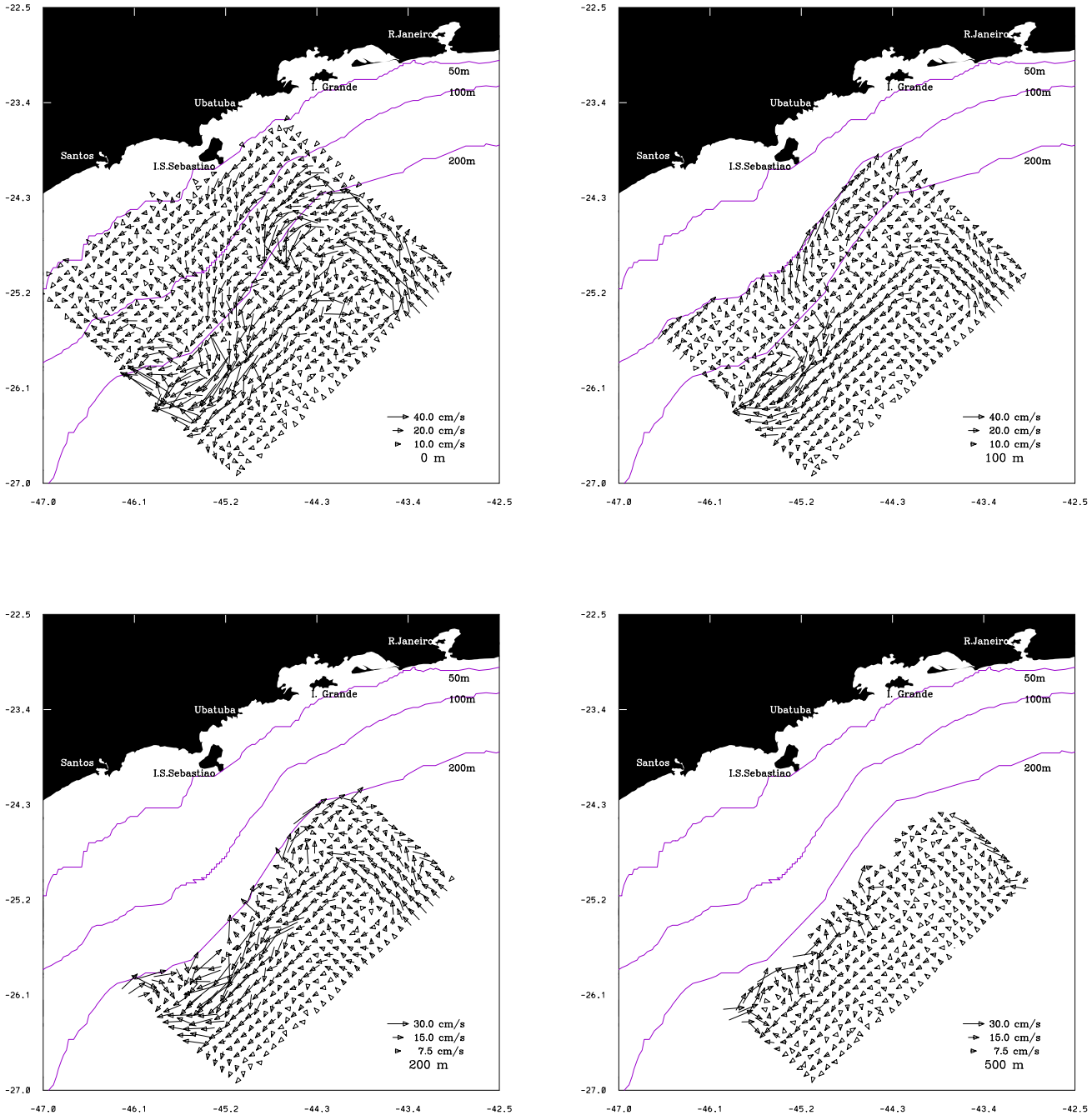
R.Janeiro
I. Grande
Ubatuba
Santos
I.S.Sebastiao
50m
100m
200m
40.0 cm/s
20.0 cm/s
10.0 cm/s
0 m
100 m
30.0 cm/s
15.0 cm/s
7.5 cm/s
200 m
500 m
-22.5
-23.4
-24.3
-25.2
-26.1
-27.0
-47.0
-46.1
-45.2
-44.3
-43.4
-42.5

Figure 7:

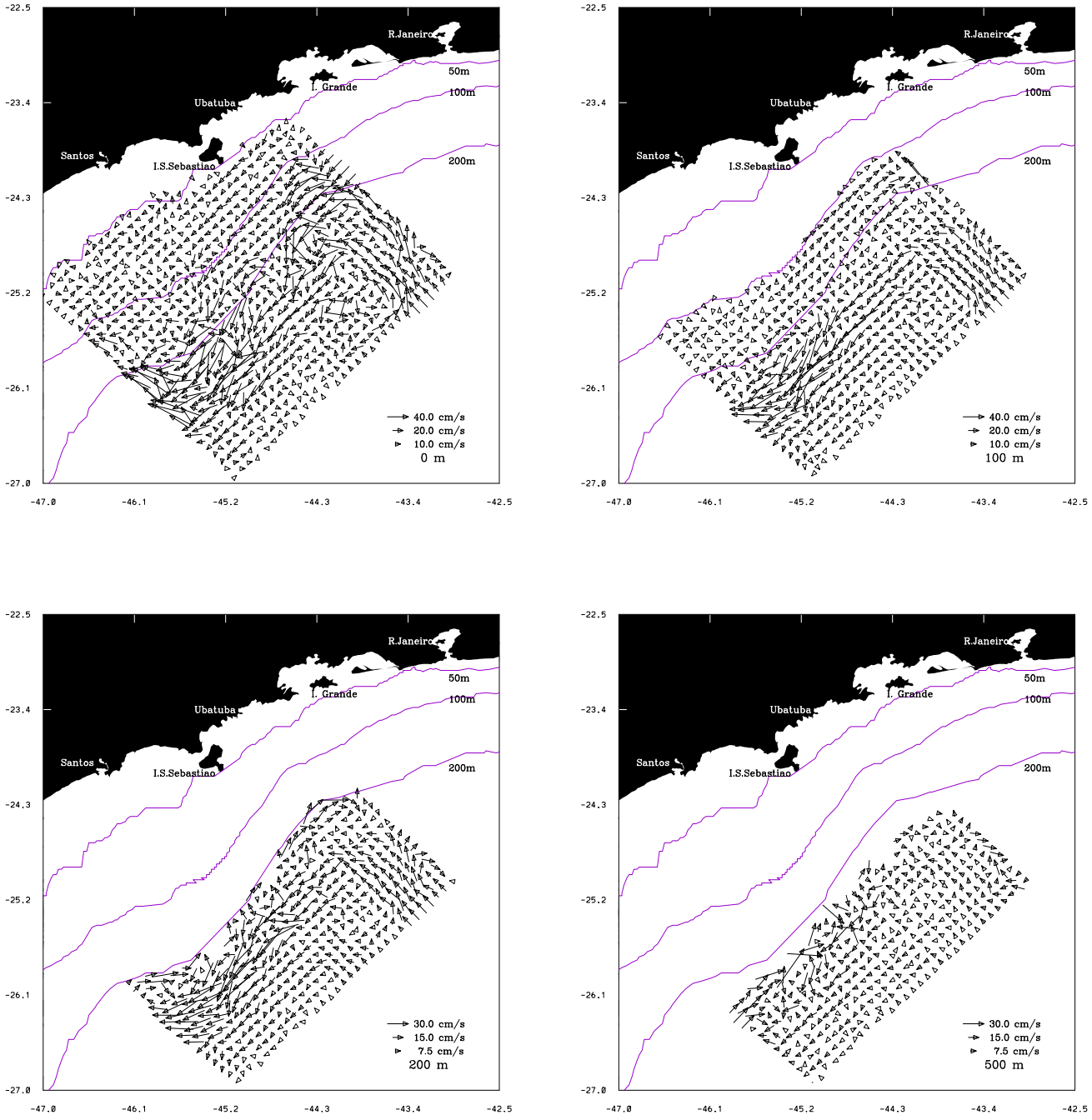
R.Janeiro
I. Grande
Ubatuba
Santos
I.S.Sebastiao
50m
100m
200m
40.0 cm/s
20.0 cm/s
10.0 cm/s
0 m
100 m
30.0 cm/s
15.0 cm/s
7.5 cm/s
200 m
500 m
-22.5
-23.4
-24.3
-25.2
-26.1
-27.0
-47.0
-46.1
-45.2
-44.3
-43.4
-42.5

Figure 8:

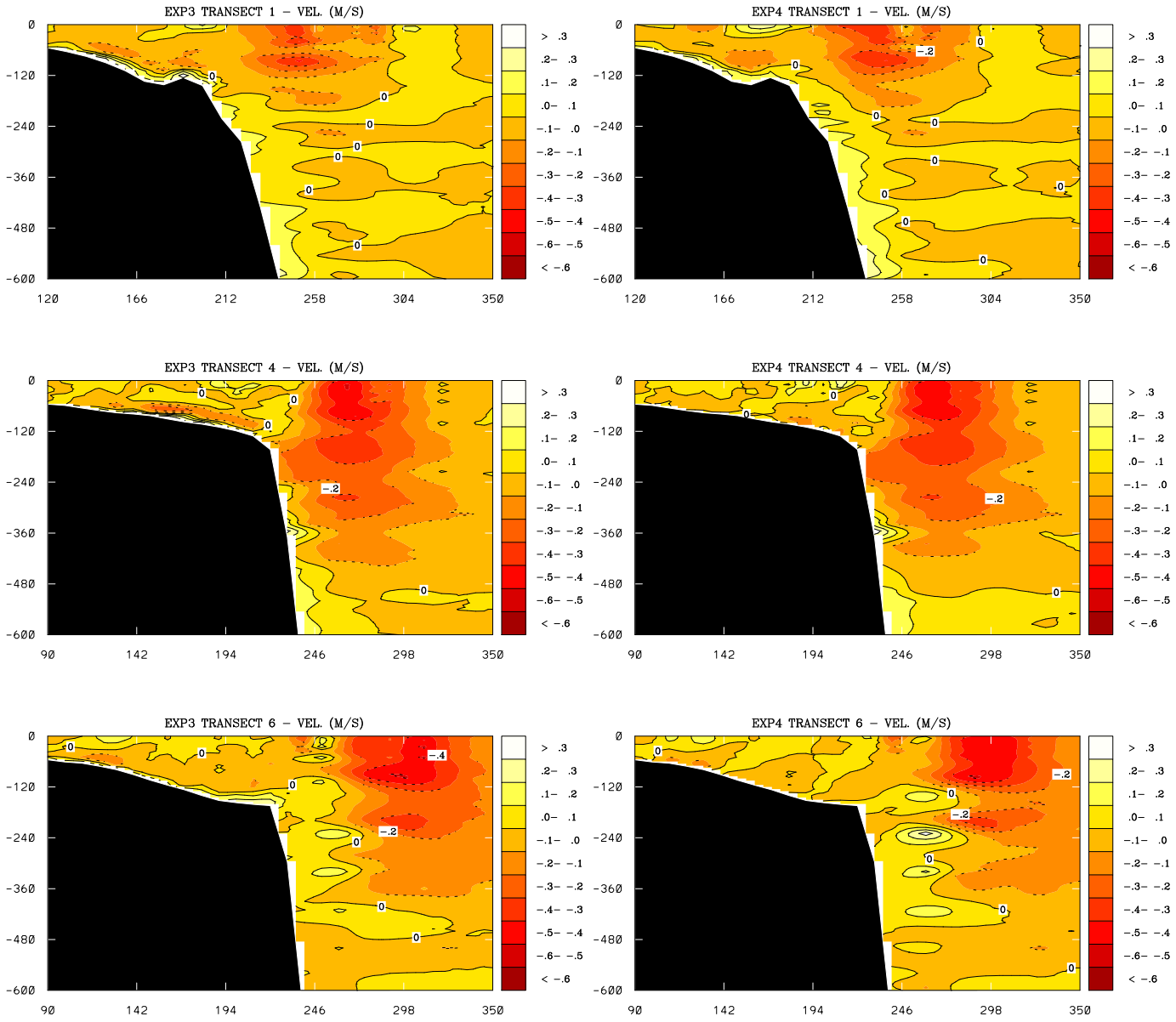
EXP3 TRANSECT 1 – VEL. (M/S)
EXP4 TRANSECT 1 – VEL. (M/S)
EXP3 TRANSECT 4 – VEL. (M/S)
EXP4 TRANSECT 4 – VEL. (M/S)
EXP3 TRANSECT 6 – VEL. (M/S)
EXP4 TRANSECT 6 – VEL. (M/S)
0
-120
-240
-360
-480
-600
120
166
212
258
304
350
90
142
194
246
298
> .3
.2– .3
.1– .2
.0– .1
–.1– .0
–.2– –.1
–.3– –.2
–.4– –.3
–.5– –.4
–.6– –.5
< –.6

Figure 9:

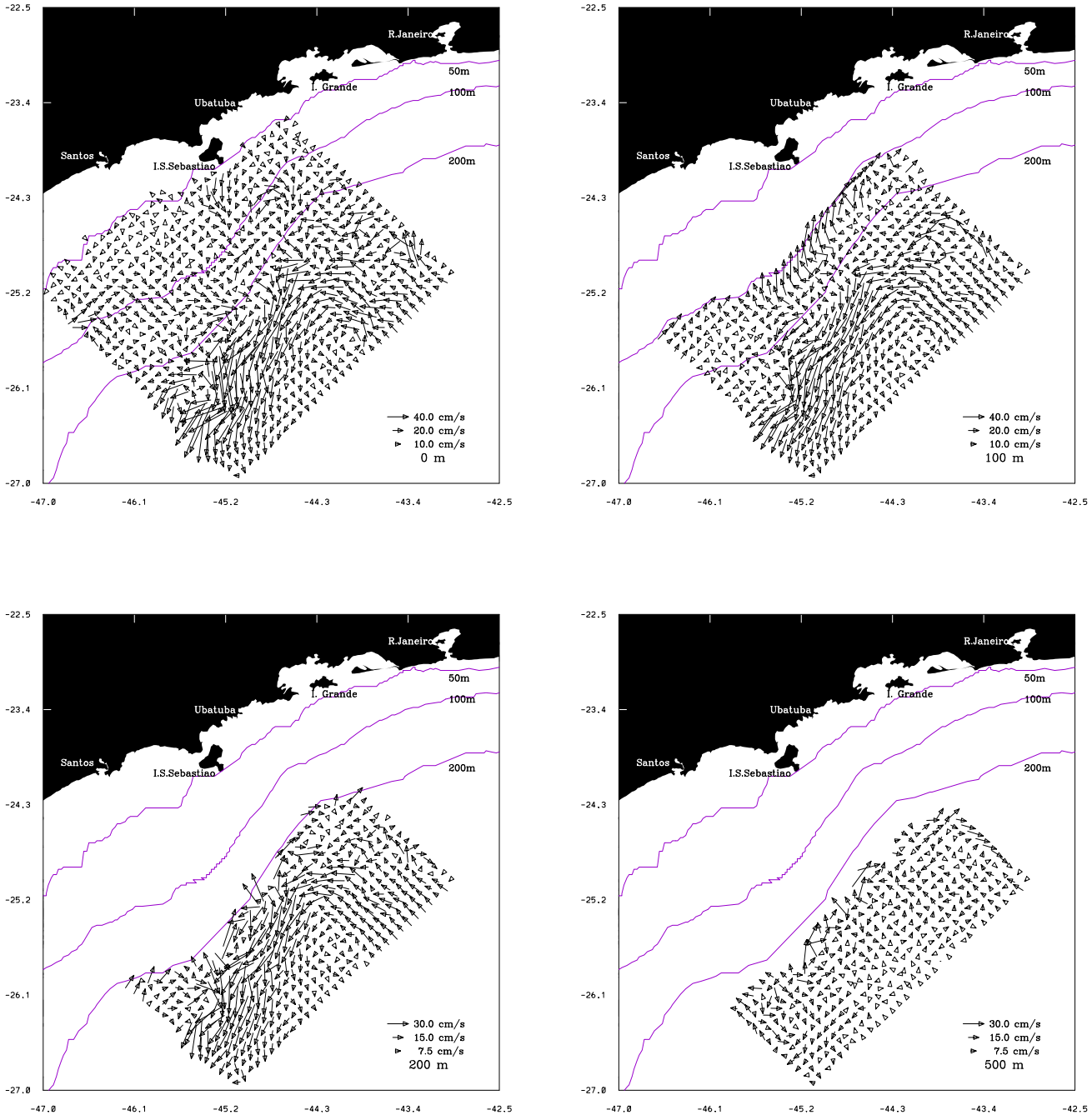
R.Janeiro
I. Grande
Ubatuba
Santos
I.S.Sebastiao
50m
100m
200m
40.0 cm/s
20.0 cm/s
10.0 cm/s
0 m
100 m
30.0 cm/s
15.0 cm/s
7.5 cm/s
200 m
500 m
-22.5
-23.4
-24.3
-25.2
-26.1
-27.0
-47.0
-46.1
-45.2
-44.3
-43.4
-42.5

Figure 10:

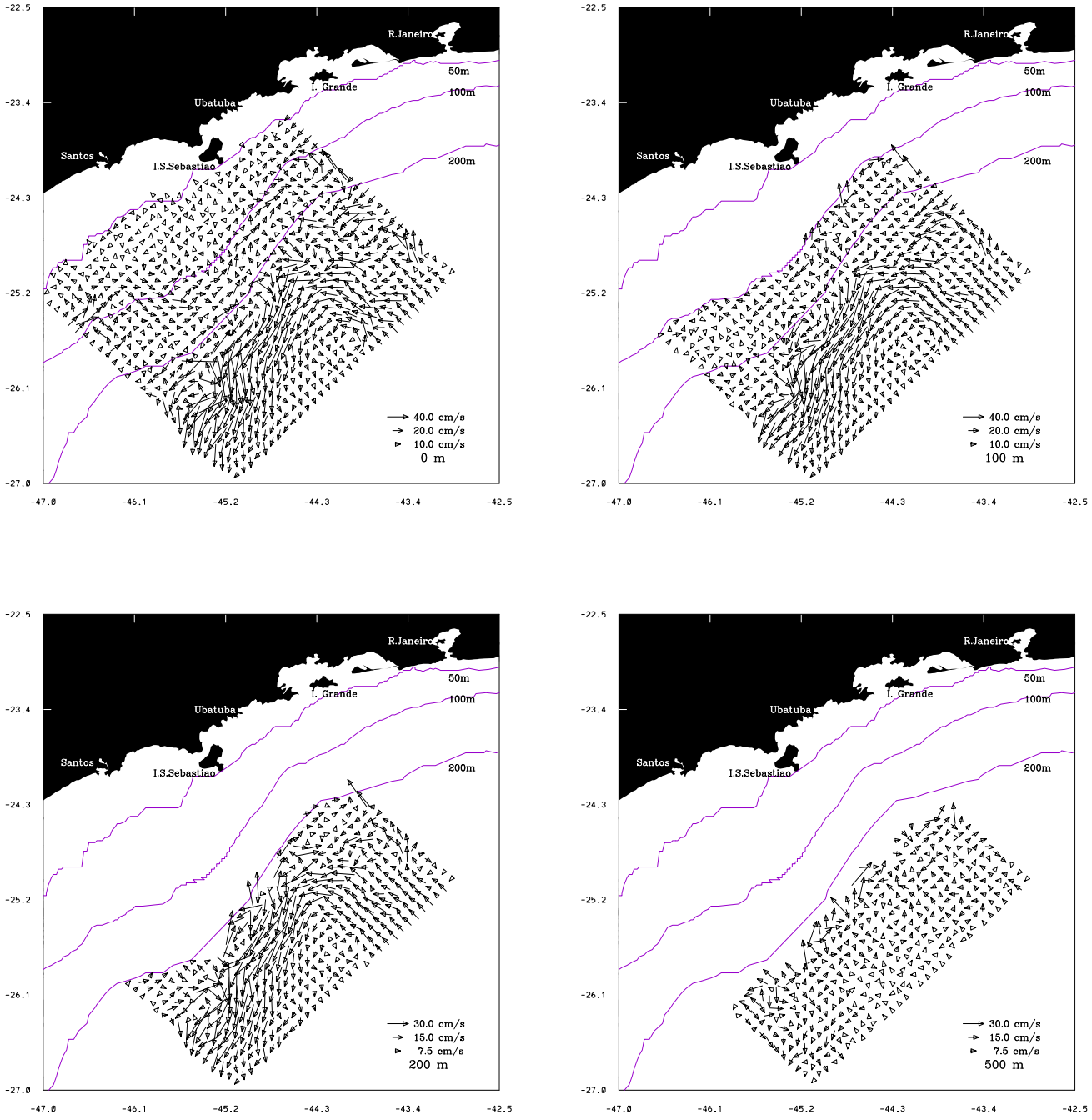
R.Janeiro
I. Grande
Ubatuba
Santos
I.S.Sebastiao
50m
100m
200m
40.0 cm/s
20.0 cm/s
10.0 cm/s
0 m
100 m
30.0 cm/s
15.0 cm/s
7.5 cm/s
200 m
500 m
-22.5
-23.4
-24.3
-25.2
-26.1
-27.0
-47.0
-46.1
-45.2
-44.3
-43.4
-42.5

Figure 11:

Level	σ	Level	σ
1	0.000	10	0.429
2	0.009	11	0.500
3	0.018	12	0.571
4	0.036	13	0.643
5	0.071	14	0.714
6	0.143	15	0.786
7	0.214	16	0.857
8	0.286	17	0.929
9	0.357	18	1.000

Table 1:

Cruise	Experiment	Description
HM1	EXP1	southward barotropic transport of 10 Sv
	EXP2	no barotropic transport
HM2	EXP3	southward barotropic transport of 10 Sv
	EXP4	no barotropic transport

Table 2: